Receptor versus counterion: capability of *N,N′*-Bis(2-aminobenzyl)-diazacrowns for giving endo- and/or exocyclic coordination of Zn^{II} [i]

Lea Vaiana, Carlos Platas-Iglesias, David Esteban-Gómez, Fernando Avecilla, Andrés de Blas* and Teresa Rodríguez-Blas†

Departamento de Química Fundamental, Facultade de Ciencias, Campus da Zapateira s/n, Universidade da Coruña, 15071 A Coruña, Spain

European Journal of Inorganic Chemistry, volume 2007, issue 13, pages 1874–1883, May 2007
Received 26 October 2006, version of record online 20 March 2007, issue online 16 April 2007

Abstract

The structure of Zn^{II} complexes with receptors L^1 and L^2[L^1 = *N,N′*-bis(2-aminobenzyl)-1,10-diaza-15-crown-5 and L^2 = *N,N′*-bis(2-aminobenzyl)-4,13-diaza-18-crown-6] was studied both in the solid state and in acetonitrile solution. Both receptors form mononuclear Zn^{II} complexes in this solvent, while no evidence for the formation of dinuclear complexes was obtained. This is in contrast with previous investigations that demonstrated the formation of dinuclear complexes of L^2 with first-row transition metals such as Ni^{II}, Co^{II} and Cu^{II}. Compounds of formula $[Zn(L^1)](ClO_4)_2$ (**1**), $[Zn(L^1)](NO_3)_2{\cdot}2CH_3CN$ (**2**), $[Zn(L^2)](ClO_4)_2$ (**3**) and $[Zn(L^2)(NO_3)_2]$ (**4**) were isolated and structurally characterised by X-ray diffraction analyses. L^1 forms seven-coordinate Zn^{II} complexes in the presence of both nitrate and perchlorate anions, as a consequence of the good fit between the macrocyclic cavity and the ionic radius of the metal ion. The Zn^{II} ion is deeply buried into the receptor cavity and the anions are forced to remain out of the metal coordination sphere. The cation $[Zn(L^1)]^{2+}$ present in **1** and **2** is one of the very few examples of seven-coordinate Zn complexes. Receptor L^2 provides a very rare example of a macrocyclic receptor allowing endocyclic and exocyclic coordination on the same guest cation, depending on the nature of the anion present. Thus, in **3** the Zn^{II} ion is endocyclically coordinated, placed inside the crown hole coordinated to four donor atoms of the ligand in a distorted tetrahedral environment, whereas in **4**, the presence of a strongly coordinating anion such as nitrate results in an exocyclic coordination of Zn^{II}, which is directly bound only to the two primarily amine groups of L^2 and two nitrate ligands. Spectrophotometric titrations of $[Zn(L^2)]^{2+}$ with tetrabutylammonium nitrate in acetonitrile solution demonstrate the stepwise formation of 1:1 and 1:2 adducts with this anion in acetonitrile solution. The $[Zn(L^1)]^{2+}$, $[Zn(L^2)]^{2+}$ and $[Zn(L^2)(NO_3)_2]$ systems were characterised by means of DFT calculations (B3LYP model). The calculated geometries show an excellent agreement with the experimental

* andres.blas@udc.es
† teresa.rodriguez.blas@udc.es

structures obtained from X-ray diffraction analyses. Calculated binding energies of the macrocyclic ligands to Zn^{II} are also consistent with the experimental data.

Keywords: zinc; macrocyclic ligands; crown compounds; coordination modes; density functional calculations

Introduction

Since Pedersen reported the synthesis and cation complexing characteristics of the crown ethers, there has been increasing interest in these compounds as complexing agents. In particular, the cyclic framework of crown ethers affords an interesting platform for the complexation of metal ions, and the ability of crown ethers to selectively coordinate metal salts has made them attractive building blocks in supramolecular chemistry and material science.[1–6] Likewise, the relative ease with which crown ethers can be functionalised with pendant arm(s) containing additional donor atom(s) allows modification of the cation-binding ability and, in some cases, the selectivity of the parent crown ether.[7] Pendant-armed crowns, also known as lariat ethers, may be regarded as having a structural character intermediate to that of a flexible macrocyclic polyether and a relatively rigid macrobicyclic cage, and the presence of additional donor atoms in the side arms can be used to enhance their coordination potential and/or to build polynuclear structures.[8] Although the coordination chemistry of crowns and armed-crown receptors has been extensively studied over the last decades,[1–4]their coordination capability is not entirely predictable.

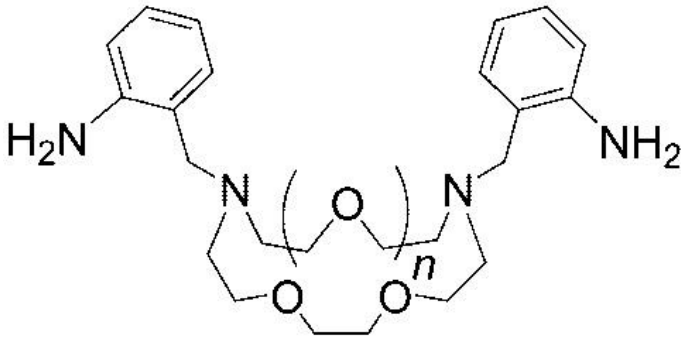

L^1: n = 1

L^2: n = 2

Scheme 1

The lariat ethers L^1 and L^2 (Scheme **1**) have been revealed as versatile receptors towards different metal ions. In some cases they impose their coordinative preferences whereas in others they adapt to steric and/or electronic requirements of the guest metal ion. In particular, we have found that whereas L^1only forms mononuclear complexes with first-row transition-metal ions such as Co^{II}, Ni^{II} and Cu^{II},[9,10] imposing a pentagonal bipyramidal geometry and so dominating over the coordinative preferences of the particular ion guest, L^2 only forms dinuclear complexes with these cations and easily adapts to the coordinative preferences of these metal ions.[10,11] In this paper we report the coordinative properties of these two lariat ethers toward Zn^{II}. It is well known that coordination properties of transition-metal complexes are mainly related to the partly filled d orbitals of the metal ion and have common types of structures with specific coordination

numbers, however, non-transition-metal complexes are able to take various coordination numbers and may show diverse structures because of the fact that d atomic orbitals of the metal centre are fully occupied. In particular, the geometries of Zn^{II} complexes can vary from tetrahedral to octahedral through trigonal-bipyramidal and square-pyramidal, all of them frequently distorted. Likewise, although rare, coordination numbers higher than six may be reached by using high denticity polydentate ligands.

The study presented in this paper provides a very rare example of a macrocyclic receptor allowing endocyclic and exocyclic coordination on the same guest cation depending on the nature of the counterion present.

Results and discussion

Synthesis and solid-state structure

The reaction of stoichiometric amounts of *N*,*N*′-bis(2-aminobenzyl)-1-10-diaza-15-crown-5 (L^1) or *N*,*N*′-bis(2-aminobenzyl)-4-13-diaza-18-crown-6 (L^2) with Zn^{II} salts (perchlorates or nitrates) in ethanol or acetonitrile solution gives compounds of formula $[Zn(L^1)](ClO_4)_2$ (**1**), $[Zn(L^1)](NO_3)_2{\cdot}2CH_3CN$ (**2**), $[Zn(L^2)](ClO_4)_2$ (**3**) and $[Zn(L^2)(NO_3)_2]$ (**4**). The FAB-mass spectrum of each complex displays very intense peaks corresponding to the $[Zn(L\text{-}H)]^+$ and $[Zn(L)(X)]^+$ fragments (L = L^1 or L^2, X = ClO_4^- or NO_3^-), thereby confirming the formation of the complexes. The IR spectra (KBr discs) of the perchlorate complexes **1** and **3** show bands corresponding to the ν_{as}(Cl–O) stretching and δ_{as}(O–Cl–O) bending modes of the perchlorate groups at about 1090 and 620 cm^{-1}. The absorption at about 620 cm^{-1} clearly shows up without splitting, as befits an uncoordinated anion.[12] The spectrum of the nitrate complex **2** exhibits an intense band at 1384 cm^{-1}, as expected for the presence of ionic nitrate.[12]

The solid-state structures of the four compounds were determined by single-crystal X-ray diffraction analysis. Crystals of **1** and **2** contain the cation $[Zn(L^1)]^{2+}$and two anions, perchlorate (**1**) or nitrate (**2**), involved in hydrogen-bonding interactions with the $–NH_2$ groups [compound **1**: N(4)···H(4B) 0.868(19) Å, H(4B)···O(9) 2.76(4) Å, N(4)···O(9) 3.209(6) Å, N(4)–H(4B)–O(9) 114(4)°; H(4B)···O(12) 2.18(2) Å, N(4)···O(12) 3.013(5) Å, N(4)–H(4B)–O(12) 162(4)°; N(3)···H(3A) 0.878(18) Å, H(3A)···O(6) 2.23(2) Å, N(3)···O(6) 3.112(7) Å, N(3)–H(3A)–O(6) 178(4)°. Compound **2**: N(2)···H(2N) 0.86(5) Å, H(2N)···O(3) 2.20(5) Å, N(2)···O(3) 2.965(5) Å, N(2)–H(2N)–O(3) 148(4)°; N(2)···H(1N) 0.79(5) Å, H(1N)···O(3) 2.56(5) Å, N(2)–H(1N)–O(3) 157(4)°]. Crystals of **2** also contain two acetonitrile molecules in the asymmetric unit. The structures of the cations present in **1** and **2** are shown in Figure **1**, while selected bond lengths and angles are given in Table **1**. The structures of both complex cations are very similar, although the one found in **2** is more symmetric and, in fact, the asymmetric unit of **2** only contains half a molecule of $[Zn(L^1)]^{2+}$. In both cases, the cation $[Zn(L^1)]^{2+}$ contains a ZnN_4O_3 core with the seven heteroatoms of L^1 coordinated to the Zn^{II} ion. The metal ion resides in the macrocyclic cavity bound by the three ether oxygen atoms and the two pivotal nitrogen atoms of the azacrown moiety, while the donor atoms of the pendant arms coordinate apically. The Zn-crown ether oxygen bonds in compounds **1** and **2** are in line with those observed for a seven-coordinate Zn^{II} complex of 15-crown-5, at an average of 2.30 Å.[13] The distances between the Zn^{II} ion and the nitrogen atoms of the aniline groups are about 0.08 Å shorter than those observed for a six-coordinate Zn^{II} complex derived from a triazamacrocycle containing three aniline pendants.[14] However, these distances are about 0.1 Å longer than those observed in the analogous d^9 complex $[Cu(L^1)]^{2+}$.[10] The N(3)–Zn–N(4) angle in **1** is 170.7(2)°, while the N(2)–Zn–N(2A) angle in **2** amounts to 175.8(2)°. Angles O(1)–Zn(1)–O(2), N(2)–Zn(1)–O(2), O(3)–Zn(1)–N(2), O(3)–Zn(1)–N(1) and N(1)–Zn(1)–O(1) in **1**, and angles O(1)–Zn(1)–N(1), O(2)–Zn(1)–N(1) and O(2)–Zn(1)–O(2A) in **2** take values close to 72° (Table **1**). Thus, the coordination sphere of the zinc ion can be described as a distorted pentagonal bipyramid with an axial compression, as the apical distances between the zinc and the donor

atoms of the pendant arms are significantly shorter than the equatorial bonds. The mean deviation from planarity of the plane containing the five equatorial donor atoms and the metal ion is relatively small, and amounts to 0.1668 Å in **1**and 0.1273 Å in **2**. In both compounds the arms of the bibracchial lariat ether $L^1$are arranged on opposite sides with respect to the crown moiety, resulting in an *anti* conformation.

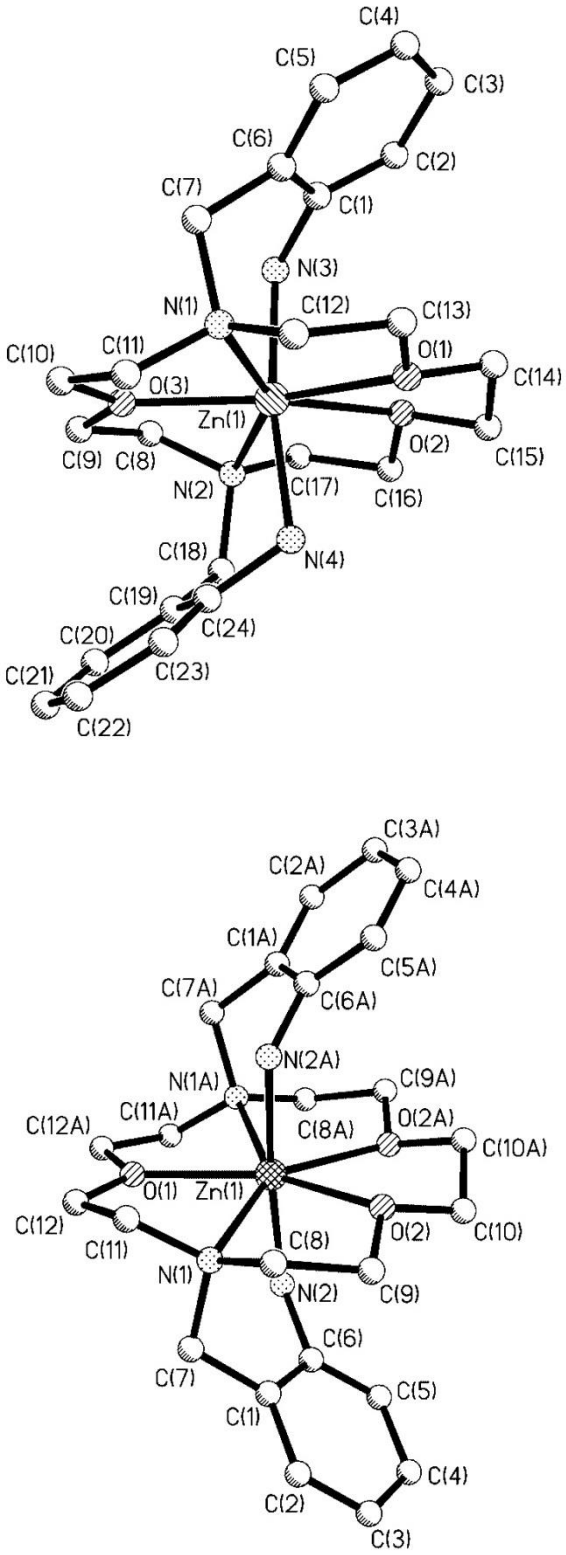

Figure 1. X-ray crystal structures of the cation $[Zn(L^1)]^{2+}$ present in compounds **1**(top) and **2** (bottom). Hydrogen atoms are omitted for simplicity. Symmetry transformations used to generate equivalent atoms in **2**: A: $-x + 1, y, -z + 3/2$.

Table 1. Selected bond lengths [Å] and angles [°] for **1** and **2**.

1		**2**[a]	
Zn(1)–N(3)	2.151(4)	Zn(1)–N(2)	2.150(3)
Zn(1)–N(4)	2.157(4)	Zn(1)–N(2A)	2.150(3)
Zn(1)–O(3)	2.172(3)	Zn(1)–O(1)	2.228(4)
Zn(1)–N(1)	2.234(4)	Zn(1)–O(2)	2.235(3)
Zn(1)–O(1)	2.281(3)	Zn(1)–O(2A)	2.235(3)
Zn(1)–N(2)	2.323(4)	Zn(1)–N(1A)	2.271(3)
Zn(1)–O(2)	2.345(3)	Zn(1)–N(1)	2.271(3)
N(3)–Zn(1)–N(4)	170.97(2)	N(2)–Zn(1)–N(2A)	175.8(2)
N(3)–Zn(1)–O(3)	91.9(2)	N(2)–Zn(1)–O(1)	92.1(1)
N(4)–Zn(1)–O(3)	96.4(2)	N(2A)–Zn(1)–O(1)	92.1(1)
N(3)–Zn(1)–N(1)	87.3(2)	N(2)–Zn(1)–O(2)	94.0(1)
N(4)–Zn(1)–N(1)	99.0(2)	N(2A)–Zn(1)–O(2)	82.6(1)
O(3)–Zn(1)–N(1)	73.4(1)	O(1)–Zn(1)–O(2)	144.8(1)
N(3)–Zn(1)–O(1)	95.4(2)	N(2)–Zn(1)–O(2A)	82.6(2)
N(4)–Zn(1)–O(1)	79.9(1)	N(2A)–Zn(1)–O(2A)	94.0(1)
N(1)–Zn(1)–O(1)	74.8(1)	O(1)–Zn(1)–O(2A)	144.8(1)
O(3)–Zn(1)–O(1)	147.0(1)	O(2)–Zn(1)–O(2A)	70.4(2)
N(3)–Zn(1)–N(2)	95.5(2)	N(2)–Zn(1)–N(1A)	95.0(1)
N(4)–Zn(1)–N(2)	83.1(2)	N(2A)–Zn(1)–N(1A)	86.4(1)
O(3)–Zn(1)–N(2)	72.8(1)	O(1)–Zn(1)–N(1A)	70.6(1)
N(1)–Zn(1)–N(2)	146.1(1)	O(2)–Zn(1)–N(1A)	142.9(2)
O(1)–Zn(1)–N(2)	138.0(1)	O(2A)–Zn(1)–N(1A)	75.2(2)
N(3)–Zn(1)–O(2)	79.8(2)	N(2)–Zn(1)–N(1)	86.4(1)
N(4)–Zn(1)–O(2)	91.0(2)	N(2A)–Zn(1)–N(1)	95.0(1)
O(3)–Zn(1)–O(2)	144.5(1)	O(1)–Zn(1)–N(1)	70.6(1)
N(1)–Zn(1)–O(2)	139.6(1)	O(2)–Zn(1)–N(1)	75.2(2)
O(1)–Zn(1)–O(2)	68.5(1)	O(2A)–Zn(1)–N(1)	142.9(2)
N(2)–Zn(1)–O(2)	73.8(1)	N(1A)–Zn(1)–N(1)	141.2(2)

[a] Symmetry transformations used to generate equivalent atoms. A: $-x + 1, y, -z + 3/2$.

Both compounds **3** and **4** contain the larger receptor L^2, and unlike the analogous compounds containing L^1, the presence of different counterions (perchlorate or nitrate) results in dramatically different coordination environments around the Zn^{II} ion. Crystals of **3** contain the $[Zn(L^2)]^{2+}$ cation and two perchlorate anions involved in hydrogen-bonding interactions with the $-NH_2$ groups [N(4)···H(2N) 0.846(19) Å, H(2N)···O(5) 2.27(4) Å, N(4)···O(5) 2.991(5) Å, N(4)–H(2N)–O(5) 171(4)°; N(3)···H(4N) 0.837(19) Å, H(4N)···O(10) 2.13(3) Å, N(3)···O(10) 2.897(6) Å, N(3)–H(4N)–O(10) 151(4)°], whereas the asymmetric unit of **4** contains a half $[Zn(L^2)(NO_3)_2]$ molecule. The structures of $[Zn(L^2)]^{2+}$ and $[Zn(L^2)(NO_3)_2]$ present in **3** and **4**, respectively, are shown in Figure **2**, while Table **2** summarises selected bond lengths and angles of the metal coordination environments. In $[Zn(L^2)]^{2+}$, the Zn^{II} ion is endocyclically coordinated but only four of the eight available donor atoms of L^2 form part of the coordination sphere. Thus, the metal ion is directly bound to both aniline pendant arms [N(3) and N(4)], one of the pivotal nitrogen atoms, N(1), and an oxygen atom of the crown, O(2), while the remaining distances between the metal ion and the other heteroatoms of the crown are too long to be considered as bond lengths [Zn–O(1) 2.498 Å; Zn–O(3) 2.596 Å; Zn–O(4) 3.464 Å; Zn–

N(2) 3.720 Å]. Receptor L^2 adopts an *anti* conformation and the coordination polyhedron around the zinc ion can be described as a distorted tetrahedron. Moreover, the $–NH_2$ group containing N(4) is involved in a hydrogen-bonding interaction with O(4) and N(2) [N(4)···H(1N) 0.80(4) Å, H(1N)···N(2) 2.27(4) Å, N(4)···N(2) 2.904(5) Å, N(4)–H(1N)–N(2) 137(3)°; N(4)···H(1N) 0.80(4) Å, H(1N)···O(4) 2.38(4) Å, N(4)···O(4) 3.063(4) Å, N(4)–H(1N)–O(4) 144(3)°].

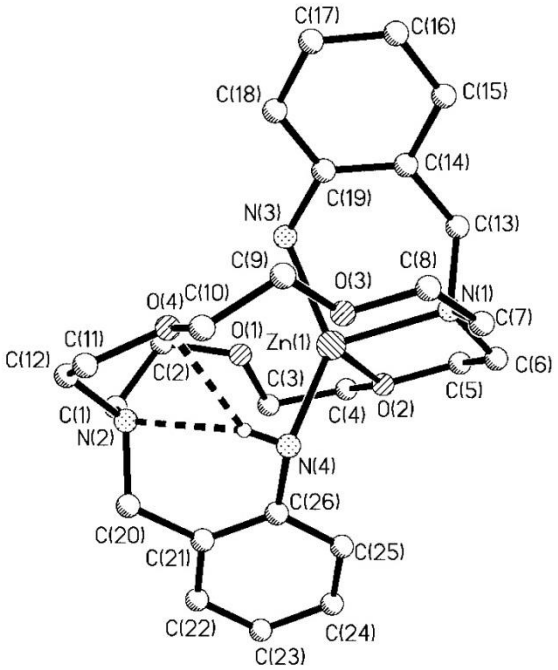

(a)

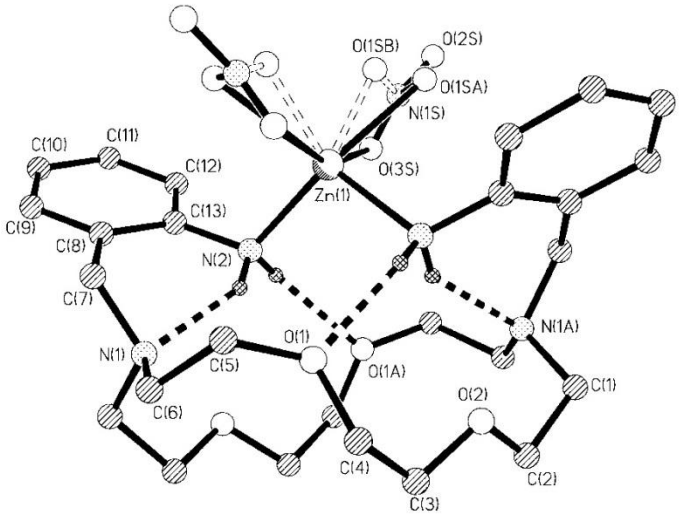

(b)

Figure 2. (a) X-ray crystal structure of the cation $[Zn(L^2)]^{2+}$ present in compound 3; (b) X-ray crystal structure of compound 4. Hydrogen atoms are omitted for simplicity. Symmetry transformations used to generate equivalent atoms in 4: #1 $–x + 2, y, –z + 1/2$.

Table 2. Selected bond lengths [Å] and angles [°] for **3** and **4**.

3	
Zn(1)–N(4)	2.014(3)
Zn(1)–N(3)	2.024(3)
Zn(1)–N(1)	2.110(3)
Zn(1)–O(2)	2.147(2)
N(4)–Zn(1)–N(3)	131.0(2)
N(4)–Zn(1)–N(1)	119.7(1)
N(4)–Zn(1)–O(2)	103.7(1)
N(3)–Zn(1)–N(1)	96.6(1)
N(3)–Zn(1)–O(2)	114.8(1)
N(1)–Zn(1)–O(2)	80.3(1)
4	
Zn(1)–N(2)	2.017(3)
Zn(1)–O(3S)	2.371(5)
Zn(1)–O(1SA)	2.336(13)
Zn(1)–O(1SB)	1.929(7)
O(1SB)#1–Zn(1)–O(1SB)	68.8(5)
O(1SB)–Zn(1)–N(2)#1	110.1(3)
O(1SB)–Zn(1)–N(2)	134.2(2)
N(2)#1–Zn(1)–N(2)	101.83(15)
N(2)–Zn(1)–O(1SA)#1	91.0(4)
N(2)–Zn(1)–O(1SA)	137.5(3)
O(1SA)#1–Zn(1)–O(1SA)	106.5(9)
O(1SB)–Zn(1)–O(3S)#1	108.2(3)
N(2)–Zn(1)–O(3S)#1	104.23(17)
O(1SA)–Zn(1)–O(3S)#1	116.5(4)
O(1SB)–Zn(1)–O(3S)	52.2(2)
N(2)–Zn(1)–O(3S)	89.09(16)
O(1SA)–Zn(1)–O(3S)	48.4(3)
O(3S)#1–Zn(1)–O(3S)	159.0(3)

[a] Symmetry transformations used to generate equivalent atoms. #1: $-x + 2, y, -z + 1/2$.

In the complex $[Zn(L^2)(NO_3)_2]$ present in **4**, the Zn^{II} ion is exocyclically coordinated with the metal ion only directly bound to the two aniline groups of L^2, [N(2)] and [N(2)#1]. The $-NH_2$ groups are also involved in an intramolecular hydrogen-bonding interaction with the pivotal nitrogen atoms and an oxygen atom of the crown moiety[N(2)···H(2A) 0.90 Å, H(2A)···O(1) 2.16 Å, N(2)···O(1) 2.993(4) Å, N(2)–H(2A)–O(1) 153.9°; N(2)···H(2B) 0.90 Å, H(2B)···N(1) 2.04 Å, N(2)···N(1) 2.825(4) Å, N(2)–H(2B)–N(1) 144.7°]. As a consequence, L^2 adopts a *syn* arrangement with both aniline pendant arms disposed on the same side of the crown. Coordination number six is completed by two nitrate ligands in a bidentate fashion, as often observed for Zn^{II} complexes with nitrate ligands.[15,16] The structure presents a disorder on one oxygen atom of a coordinated nitrate group and, as a result, the bidentate nitrate ion is coordinated in a nearly symmetrical fashion [Zn(1)–O(1SA) 2.336(13) Å, Zn(1)–O(3S) 2.371(5) Å] or in a clearly asymmetrical one [Zn(1)–O(1SB) 1.929(7) Å, Zn(1)–O(3S) 2.371(5) Å], depending on the occupation of sites O(1SA) or O(1SB).

A comparison of the bond lengths of the metal coordination environment in $[Zn(L^1)]^{2+}$ present in compounds **1** and **2** with those observed for $[Zn(L^2)]^{2+}$present in **3** clearly shows a shortening of the bond lengths as the coordination number of the metal ion decreases. Likewise, the distances between the Zn^{II} ion and the nitrogen atoms of the aniline groups in compounds **3** and **4** are close to those observed in four-coordinate Zn^{II} complexes containing aniline groups.[17,18]

Solution behaviour

The behaviour in $[D_3]$acetonitrile solution of compounds **1**–**4** was investigated by ^{1}H NMR spectroscopy. Significant changes in the chemical shifts, the structures of the signals and even the number of signals are observed in the ^{1}H NMR spectra upon coordination of the receptors to Zn^{II}. The most complicated region of the spectra is that where the ethylene and methylene proton signals are observed. The coordination to the metal ion increases the rigidity of the receptor, limiting conformational exchange processes, so that the geminal CH_2 protons are no longer equivalent. The aromatic region usually appears more clearly resolved in all complexes except for the nitrate complex **4** because of the presence of a conformational equilibrium between the different species present in solution (see Figure **3**).

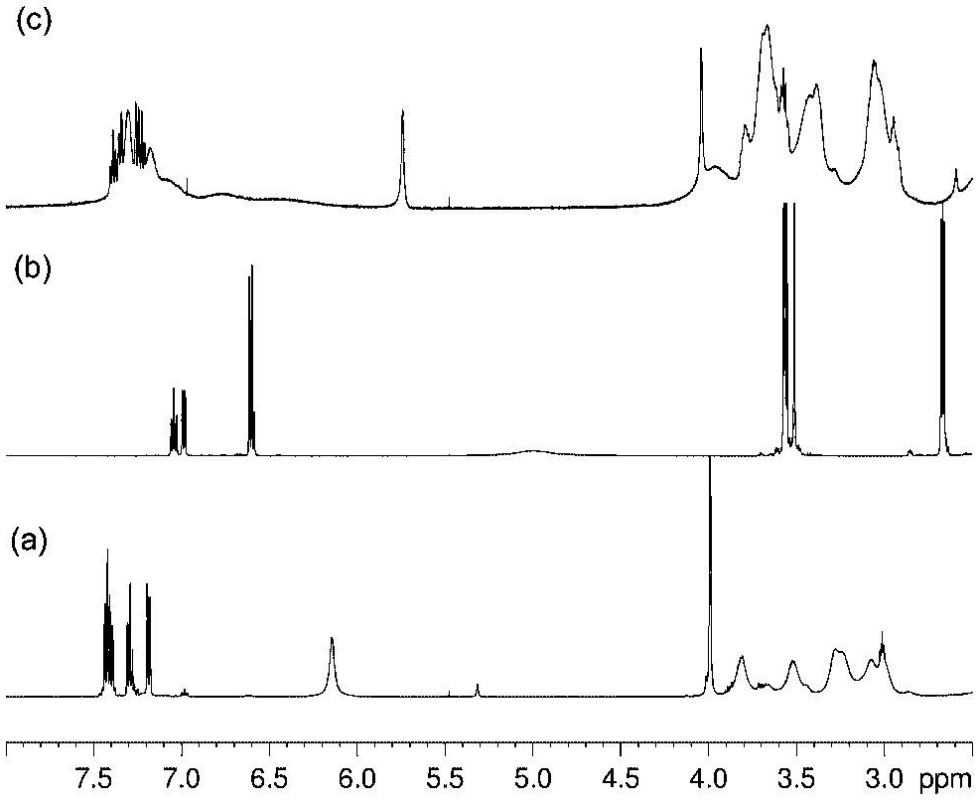

Figure 3. ^{1}H NMR spectra recorded at 298 K on 10^{-3} M solutions of 3 (spectrum a), L^2 (spectrum b) and 4 (spectrum c).

The ^{1}H NMR spectra of compounds **1** and **2** are identical, indicating that the presence of different counterions (perchlorate or nitrate) does not affect the structure of the $[Zn(L^1)]^{2+}$ cation in solution. The signals corresponding to the protons of the aromatic units are shifted downfield by about 0.4–0.6 ppm upon coordination to the metal ion, thereby confirming the coordination of the ligand to the metal ion in this solvent (Figures S1 and S2, Supporting Information). Conductivity measurements carried out in acetonitrile solution (281 Ω^{-1} cm^2 mol^{-1}for **1** and 194 Ω^{-1} cm^2 mol^{-1} for **2**) show that **1** and **2** behave as 2:1 electrolytes in

this solvent,[19] confirming that the nature of the counterion has no influence in the coordination sphere of the metal ion, in agreement with their solid-state structures. The situation is quite different for compounds **3** and **4**. The molar conductivity measured for **3** in acetonitrile solution (287 Ω^{-1} cm^2 mol^{-1}) indicates that this compound behaves as a 2:1 electrolyte in this solvent, while the molar conductivity determined for a solution of **4** (prepared in situ by mixing stoichiometric amounts of L^2 and Zn^{II} nitrate) is clearly lower (134 Ω^{-1} cm^2 mol^{-1}). These results are in agreement with the coordination of the NO_3^- ligands to the metal ion. The interaction of $[Zn(L^2)]^{2+}$ is, however, relatively weak (vide infra), and therefore the conductivity measured experimentally is an average of the conductivity values of the different species in equilibrium. The ^{1}H NMR spectra of **3** and **4** show that the signals of protons of the aromatic and amine groups are shifted downfield with respect to their position in the spectrum of the free receptor, indicating the coordination of the receptor to the metal ion in both compounds. However, while these signals are well resolved in the case of compound **3**, the spectrum of **4** shows broad resonances between 6.5 and 7.5 ppm (Figure **3**). This is probably due to the presence in solutionof exchange processes involving $[Zn(L^2)(NO_3)_2]$, $[Zn(L^2)(NO_3)]^+$ and $[Zn(L^2)]^{2+}$ complex species (vide infra). The spectra of **3** and **4** are very different (Figure **3**), indicating a different structure of the complexes in solution, as also observed in the solid state. This is confirmed by a ^{1}H NMR titration experiment, where tetrabutylammonium nitrate was added to a solution of compound **3** (Figure S3, Supporting Information). During the titration the aromatic proton signals gradually shifted upfield, giving rise to an identical spectral pattern to that observed for compound **4**. Upon addition of increasing amounts of NO_3^-, the intensity of the sharp signals due to the $[Zn(L^2)]^{2+}$ species gradually decrease as a new set of broad signals appear, in agreement with the formation of the $[Zn(L^2)(NO_3)_2]$ complex.

The UV/Vis spectra of L^1 and L^2 show two absorption bands at 240 and 290 nm, resulting from the $\pi \rightarrow \pi^*$ andn $\rightarrow \pi^*$ transitions on the aromatic subunits of the ligand. Upon addition of Zn^{II} perchlorate both absorption bands show a blueshift while their intensity decreases. Figure **4** shows the spectral changes observed during the formation of the Zn^{II} complexes of L^1 and L^2. The data display a single inflection point when the M/ligand molar ratio is close to 1, indicating a 1:1 reaction stoichiometry. The steep curvature of the titration profiles corresponds to an especially high equilibrium constant ($\log K > 7$). In particular, the *p*parameter (*p* = [concentration of complex]/[maximum possible concentration of complex]) was found to be higher than 0.8 in both cases, a condition that does not permit the determination of a reliable equilibrium constant.[20] A similar situation was observed for the Mn^{II}, Co^{II} and Ni^{II} complexes of L^1.[9] It is interesting to note that while L^2 is able to form dinuclear complexes with metal ions such as Co^{II}, Ni^{II}[11] and Cu^{II}[10] no evidence has been obtained in this work for the formation of analogous dinuclear Zn^{II} complexes at room temperature. The UV/Vis spectrum of $\mathbf{L^2}$ recorded in the presence of a 10 fold excess of Zn^{II} does not change when the solution is heated to reflux for 24 h, indicating that no dinuclear species are formed even under these conditions.

The addition of tetrabutylammonium nitrate to a solution of $[Zn(L^2)]^{2+}$ provokes a substantial variation of the UV/Vis spectrum (Figure **5**). Upon addition of NO_3^- the intensity of the band that the complex shows at 290 nm increases. This is in agreement with the formation of the exocyclic complex because of the coordination of NO_3^- to the metal ion. Indeed, the X-ray structure of **4** shows that the Zn^{II} ion is not coordinated to the pivotal nitrogen atoms of the macrocycle, while at least one of the pivotal nitrogen atoms is involved in the coordination to Zn^{II} in **3**. Thus, the decoordination of the pivotal nitrogen atoms appears to provoke an increase of the intensity of the band at 290 nm, in line with the spectral variations observed during the formation of complexes $[Zn(L^1)]^{2+}$ and $[Zn(L^2)]^{2+}$. The titration profile shown in the inset of Figure **5** indicates the formation of at least two complex species in solution.

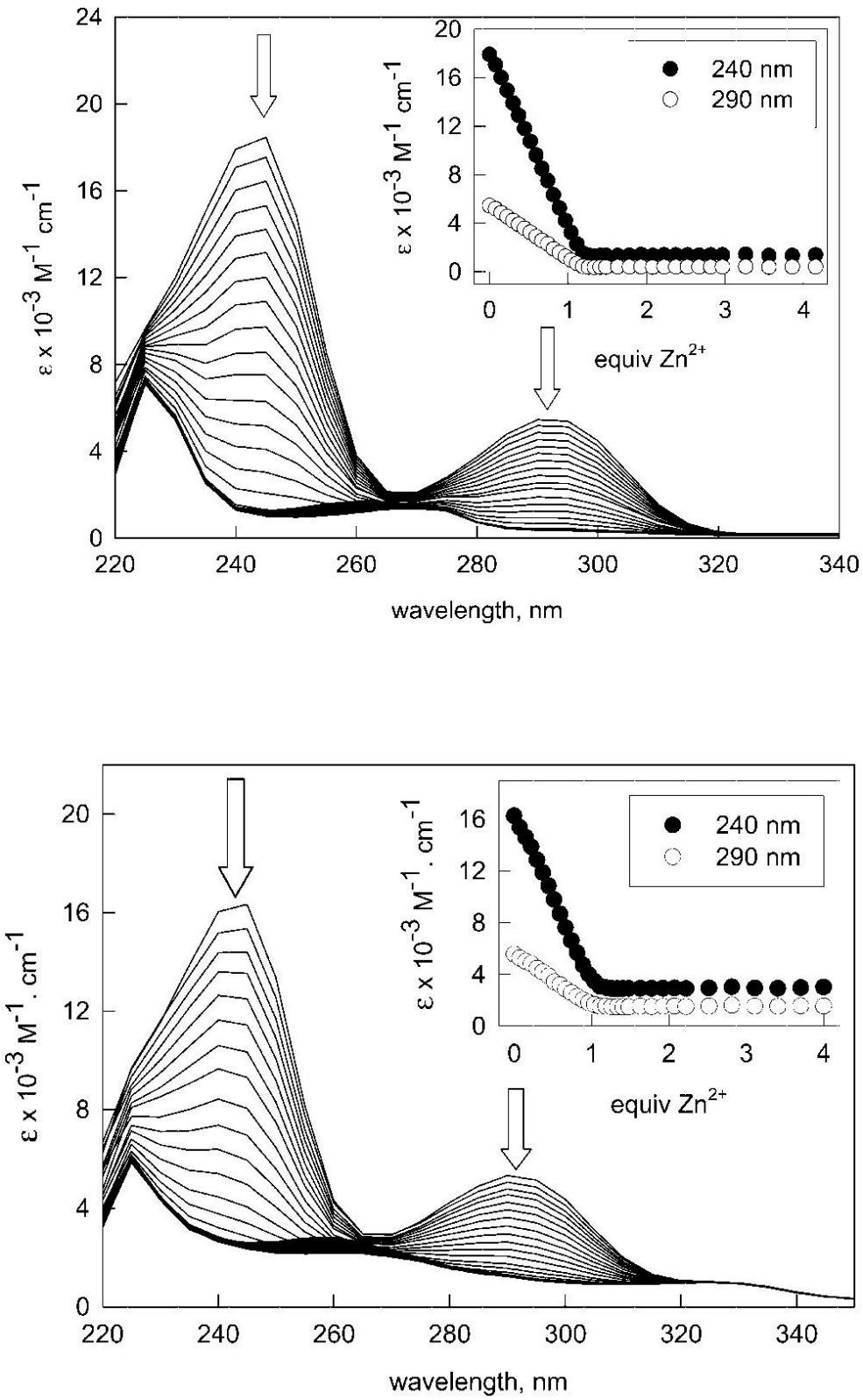

Figure 4. UV/Vis spectrum of L^1 (top) and L^2 (bottom) in acetonitrile solution and spectral changes upon addition of aliquots of a solution of $Zn(ClO_4)_2 \cdot 6H_2O$ in the same solvent.

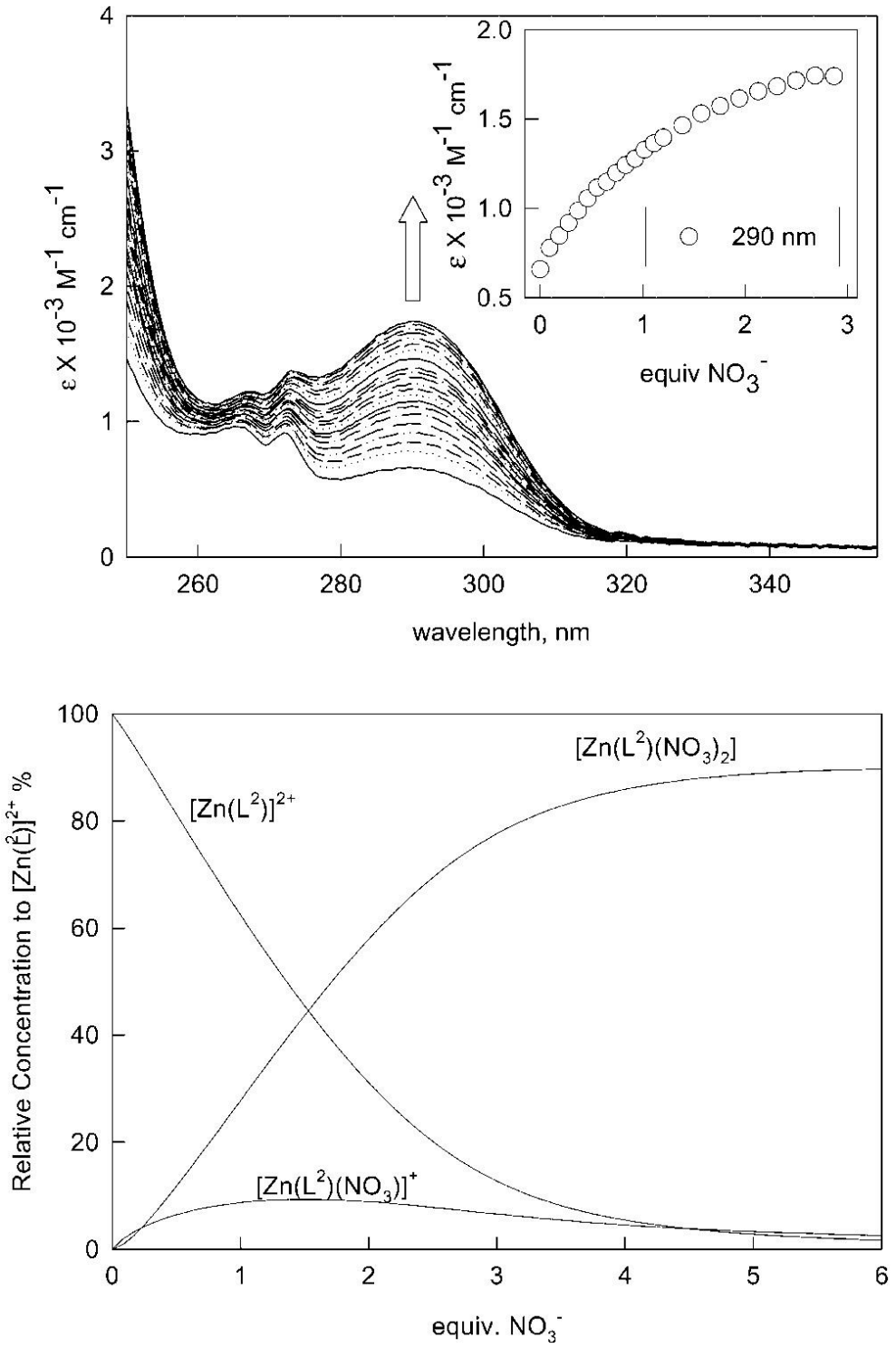

Figure 5. Top: UV/Vis spectrum of $[Zn(L^2)]^{2+}$ in acetonitrile solution and spectral changes upon addition of aliquots of a solution of tetrabutylammonium nitrate in the same solvent. Bottom: Species distribution diagram obtained from the best fit of the experimental data (see text).

$$[Zn(L^2)]^{2+} + NO_3^- \leftrightarrows [Zn(L^2)(NO_3)]^+ \qquad \beta_{11}$$

$$[Zn(L^2)]^{2+} + 2\,NO_3^- \leftrightarrows [Zn(L^2)(NO_3)_2] \qquad \beta_{12}$$

The best fit of the experimental data gives $\log \beta_{11} = 3.57(2)$ and $\log \beta_{12} = 8.5(1)$. These results indicate the stepwise formation of 1:1 and 1:2 adducts during the course of the titration. Figure **5** shows how the concentration of the species at the equilibrium, calculated from β_{11} and β_{12} values, varies upon nitrate addition. It can be seen that, because of the especially high value of β_{12}, the neutral complex $[Zn(L^1)(NO_3)_2]$ is formed in the early stages of titration. Notice also that under the conditions of the UV/Vis titration experiment the highest concentration of $[Zn(L^1)(NO_3)]^+$ is about 9 %, reached after the addition of 1.6 equiv. of NO_3^-.

DFT studies

Density functional theory (DFT) has emerged as the computational method of choice for the solution of many chemical problems. This is because DFT methods have relatively low computational cost, include a significant amount of the dynamic electron correlation and are applicable to a wide range of molecular types, including Zn^{II} complexes.[21] In a recent paper we reported a theoretical study of the $[M(L^1)]^{2+}$ systems (M = Mn, Co or Ni) at the DFT (B3LYP) computational level.[9] The calculated geometries obtained from geometry optimisations for those systems show an excellent agreement with the experimental structures obtained by X-ray diffraction analyses. Moreover, a molecular orbital analysis on the calculated structures allowed us to gain insight into the electronic structure of this family of complexes. Aiming to understand if analogous calculations can reproduce the experimental structures reported in this paper, we have performed DFT calculations on the complexes reported in this work by using the B3LYP model. Full geometry optimisations of the $[Zn(L^1)]^{2+}$, $[Zn(L^2)]^{2+}$ and $[Zn(L^2)(NO_3)_2]$ systems were performed in vacuo by using the standard 6-31G(d) basis on the ligand atoms and Ahlrichs' valence triple-ζ (VTC) on Zn.[22] The latter basis has been shown to provide accurate molecular structures for several first-row transition-metal complexes.[23]

The most relevant geometrical parameters calculated for $[Zn(L^1)]^{2+}$, $[Zn(L^2)]^{2+}$ and $[Zn(L^2)(NO_3)_2]$ systems are given in Table S1 (Supporting Information). The calculated bond lengths for $[Zn(L^1)]^{2+}$ are in excellent agreement with those observed experimentally for compound **2**, as evidenced by the excellent agreement factor obtained (Table **3**, $AF_i = [(\text{exp} - \text{calcd})^2/(\text{exp})^2]^{1/2}$, where exp and calcd denote experimental and calculated values, respectively).[24,25] Calculated bond lengths of the metal coordination environment deviate from the experimental distances determined for **2** by less than 0.07 Å, while calculated bond angles of the Zn^{II} coordination environment deviate by less than 4.0° from the experimental values. Although no geometrical constraints were used during the geometry optimisation, the calculated structure of $[Zn(L^1)]^{2+}$ corresponds to a nearly undistorted C_2 symmetry that shows a slightly better agreement with the X-ray structure of **2** than with that of compound **1** (Table **3**). The agreement factors between calculated and experimental geometrical parameters obtained for $[Zn(L^2)]^{2+}$ indicate that the experimental geometry is well reproduced at the B3LYP/6-31G(d) level, calculated bond lengths deviating from experimental values by less than 0.04 Å. For $[Zn(L^2)(NO_3)_2]$ our calculations provide a poorer agreement with experimental data than for $[Zn(L^1)]^{2+}$ and $[Zn(L^2)]^{2+}$ (Table **3**). However, this is not surprising because the X-ray crystal structure of compound **4**shows that the coordinated nitrate anions are disordered, which suggests a rather shallow potential-energy surface for the variation of the Zn–O bond lengths. In the calculated structure the nitrate anions are coordinated in a nearly symmetrical fashion [Zn(1)–O(1S) 2.178 Å, Zn(1)–O(3S) 2.107 Å].

The metal cation–ligand binding energies are summarised in Table **3**. In these calculations the basis-set superposition error (BSSE) was taken into account by the counterpoise method.[26] BSSE corrections are of similar magnitude for the three systems and do not change the calculated order of binding energies. The results predict a stronger interaction of the macrocyclic ligand with Zn^{II} for L^1than for L^2, in agreement with the results from the spectrophotometric titrations. This stronger interaction can be attributed to a better fit of the cation in the macrocyclic cavity of L^1 than in that of L^2. The lower coordination number of the metal ion in $[Zn(L^2)(NO_3)_2]$, where Zn^{II} is exocyclically coordinated and only bound to the two nitrogen atoms of the aniline groups of the receptor L^2, results in a very low binding energy for this one (50.5 kcal mol^{-1}), while

the binding energy of the two nitrate ligands is much higher (396.2 kcal mol^{-1}). These results indicate a strong interaction of the nitrate anions with Zn^{II}, while the interaction of the metal ion with the macrocyclic ligand appears to be very weak.

Table 3. Agreement factors (AF_i)[a] between exp./calcd. bond lengths and angles of the metal coordination environment for $[Zn(L^1)]^{2+}$, $[Zn(L^2)]^{2+}$ and $[Zn(L^2)(NO_3)_2]$, binding energies of the macrocyclic ligands [kcal mol^{-1}] and basis-set superposition error corrections [kcal mol^{-1}].

	$Zn(L^1)]^{2+}$	$[Zn(L^2)]^{2+}$	$[Zn(L^2)(NO_3)_2]$
AF_i (bond lengths)	0.026[b]/0.021[c]	0.016	0.083[d]/0.102[e]
AF_i (bond angles)	0.032[b]/0.018[c]	0.067	0.093[d]/0.106[e]
Binding energy[f]	412.5	405.9	50.5
BSSE[f]	7.8	7.3	20.6

[a] $AF_i = [(\text{exp.} - \text{calcd.})^2/(\text{exp.})^2]^{1/2}$. [b] Experimental data from the X-ray structure of **1**. [c] Experimental data from the X-ray structure of **2**. [d] Calculated by using O(1SA). [e] Calculated by using O(1SB). [f] Binding energies include corrections for basis-set superposition error (BSSE).

Conclusions

Zn^{II} binding by the lariat crown ethers L^1 and L^2 [L^1 = *N*,*N*′-bis(2-aminobenzyl)-1,10-diaza-15-crown-5 and L^2 = *N*,*N*′-bis(2-aminobenzyl)-4,13-diaza-18-crown-6] was analysed by spectrophotometric measurements in acetonitrile solution. Both receptors form stable mononuclear Zn^{II} complexes in this solvent, while no evidence for the formation of dinuclear complexes was obtained. L^1 forms seven-coordinate Zn^{II} complexes in the presence of both nitrate and perchlorate anions, as a consequence of the good fit between the macrocyclic cavity and the ionic radius of the metal ion. The Zn^{II} ion is deeply buried in the receptor cavity and the anions are forced to remain out of the metal coordination sphere. The cation $[Zn(L^1)]^{2+}$ is one of the very few examples of seven-coordinate Zn complexes. In fact, a recent estimate based on the number of transition-metal σ-bonded complexes found in the Cambridge Structural Database reveals that seven-coordinate complexes represent 1.8 % of the total number of structures reported and, even more, the distribution of seven-coordination throughout the first metal transition series is also quite irregular and it appears to be more common for manganese, iron and cobalt, than for zinc.

On the other hand, the cavity of L^2 is rather large for Zn^{II}, so that different coordination environments are observed for the metal cation depending on the coordinative properties of the counterion. The X-ray structure of the perchlorate salt **3** shows the metal ion placed inside the crown hole coordinated to four donor atoms of the ligand in a distorted tetrahedral environment, whereas the presence of a strongly coordinating anion such as nitrate results in an exocyclic coordination of Zn^{II}, which is directly bound only to the two primary amine groups of L^2. Spectrophotometric titrations of $[Zn(L^2)]^{2+}$ with NO_3^- also indicate an exocyclic coordination of the metal ion in acetonitrile solution. DFT calculations performed at the B3LYP level reproduce the experimental structures of the $[Zn(L^1)]^{2+}$, $[Zn(L^2)]^{2+}$ and $[Zn(L^2)(NO_3)_2]$ systems obtained by X-ray diffraction analysis fairly well. They also predict a stronger binding of L^1 to Zn^{II} compared to L^2.

The ability of a macrocyclic receptor to give endocyclic and exocyclic coordination on the same guest cation depending on the nature of the anion present in the medium is very rare. Although some examples with S-containing macrocycles and soft metals such as Pd^{II} have been reported,[27] to the best of our knowledge compounds **3** and **4** reported here represent the first example of this with a pendant-armed crown and Zn^{II}.

Experimental section

Materials and synthesis: *N*,*N*′-Bis(2-aminobenzyl)-1,10-diaza-15-crown-5 (L^1)[28] and *N*,*N*′-bis(2-aminobenzyl)-4,13-diaza-18-crown-6 (L^2)[10] were prepared as previously reported by us. All other chemicals were purchased from commercial sources and used without further purification. Solvents were of reagent grade purified by the usual methods.

Caution! *Perchlorate salts combined with organic ligands are potentially explosive and should be handled in small quantities and with the necessary precautions.*[29]

$[Zn(L^1)](ClO_4)_2$ (1): A mixture of L^1 (0.100 g, 0.233 mmol) and $Zn(ClO_4)_2 \cdot 6H_2O$ (0.087 g, 0.233 mmol) in ethanol (23 mL) was stirred and heated to reflux over a period of 8 h. The white precipitate formed was isolated by filtration and air-dried (0.152 g, 94 %). $C_{24}H_{36}Cl_2N_4O_{11}Zn$ (692.86): calcd. C 41.6, H 5.2, N 8.1; found C 41.3, H 5.1, N 8.0. FAB-MS: *m*/*z* (%BPI) = 591 (41) $[Zn(L^1)(ClO_4)]^+$, 491 (100) $[Zn(L^1 - H)]^+$. FTIR (KBr): $\tilde{\nu}$ = 3340 [$\nu_{as}(NH_2)$], 3250 [$\nu_s(NH_2)$], 1617 [$\delta(NH_2)$], 1586 [ν(C=C)], 1078 [ν_{as}(Cl–O)], 620 [δ_{as}(Cl–O)] cm^{-1}. Λ_M (acetonitrile, $cm^2\,\Omega^{-1}\,mol^{-1}$): 281 (2:1 electrolyte). Slow diffusion of diethyl ether into a solution of **1** in acetonitrile gave single crystals suitable for X-ray crystallography.

$[Zn(L^1)](NO_3)_2 \cdot 2CH_3CN$ (2): A mixture of L^1 (0.104 g, 0.243 mmol) and $Zn(NO_3)_2 \cdot 6H_2O$ (0.075 g, 0.253 mmol) in acetonitrile (20 mL) was stirred and heated to reflux over a period of 6 h. Slow diffusion of diethyl ether into the former solution at room temperature produced colourless crystals that were collected by filtration and air-dried (0.097 g, 57 %). $C_{28}H_{42}N_8O_9Zn$ (700.07): calcd. C 48.0, H 6.1, N 15.6; found C 47.1, H 6.1, N 16.0. FAB-MS: *m*/*z* (%BPI) = 491 (28) $[Zn(L^1 - H)]^+$. FTIR (KBr): $\tilde{\nu}$ = 3268, 3225 [$\nu_{as}(NH_2)$], 3123, 3090 [$\nu_s(NH_2)$], 1618 [$\delta(NH_2)$], 1591 [ν(C=C)], 1384 [$\nu(NO_3)$] cm^{-1}. Λ_M (acetonitrile, $cm^2\,\Omega^{-1}\,mol^{-1}$): 194 (2:1 electrolyte). Slow diffusion of diethyl ether into a solution of **2** in acetonitrile gave single crystals suitable for X-ray crystallography.

$[Zn(L^2)](ClO_4)_2$ (3): The preparation of the white complex followed the same procedure as for **1** by using L^2 (0.107 g, 0.226 mmol) and $Zn(ClO_4)_2 \cdot 6H_2O$ (0.085 g, 0.228 mmol) in ethanol (23 mL) (0.125 g, 75 %). $C_{26}H_{40}Cl_2N_4O_{12}Zn$ (736.91): calcd. C 42.4, H 5.5, N 7.6; found C 42.0, H 5.5, N 7.5. FAB-MS: *m*/*z* (%BPI) = 635 (28) $[Zn(L^2)(ClO_4)]^+$, 535 (58) $[Zn(L^2 - H)]^+$, 473 (100) $[L^2 + H]^+$. FTIR (KBr): $\tilde{\nu}$ = 3225 [$\nu(NH_2)$], 1614 [$\delta(NH_2)$], 1589 [ν(C=C)], 1092 [ν_{as}(Cl–O)], 622 [δ_{as}(Cl–O)] cm^{-1}. Λ_M(acetonitrile, $cm^2\,\Omega^{-1}\,mol^{-1}$): 287 (2:1 electrolyte). Slow diffusion of diethyl ether into a solution of **3** in acetonitrile gave single crystals suitable for X-ray crystallography.

$[Zn(L^2)(NO_3)_2]$ (4): Slow diffusion of diethyl ether into a solution of $Zn(NO_3)_2 \cdot 6H_2O$ (0.067 g, 0.225 mmol) and L^2 (0.105 g, 0.222 mmol) in acetonitrile (7 mL) gave some single crystals suitable for X-ray crystallography. Attempts to isolate more compound **4** were unsuccessful because it formed an intractable oily product when separated from the solvent.

Physical measurements: Elemental analyses were carried out on a Carlo–Erba 1180 elemental analyser. FAB mass spectra were recorded with a Fisons Quatro mass spectrometer with a Cs ion gun using 3-nitrobenzyl alcohol as matrix. IR spectra were recorded, as KBr discs, using a Bruker Vector 22 spectrophotometer. Conductivity measurements were carried out at 20 °C with a Crison Micro CM 2201 conductimeter using 10^{-3} M solutions of the complexes in acetonitrile. ^{1}H NMR spectra were run on a Bruker AC 200 F or a Bruker WM-500 spectrometer. Proton NMR titration was performed on 5×10^{-3} M solution of **3** and in [D_3]acetonitrile. Typically, aliquots of a fresh tetrabutylammonium nitrate solution (0.5 M) were added, and the ^{1}H NMR spectra of the samples were recorded.

Spectrophotometric titrations: UV/Vis spectra were recorded with Hewlett–Packard 8452A or Perkin–Elmer Lambda 900 spectrophotometers, with a quartz cell (path length: 10 cm). The cell holder was thermostatted at 25.0 °C through circulating water. Spectrophotometric titrations were performed at 25 °C on 5.0×10^{-5} M

solutions of L^1 or L^2 in MeCN (polarographic grade). Typically, aliquots of a fresh $Zn(ClO_4)_2 \cdot 6H_2O$ standard solution were added and the UV/Vis spectra of the samples were recorded. The spectrophotometric titration of $[Zn(L^2)]^{2+}$ with tetrabutylammonium nitrate was performed on a 1×10^{-5} M solution of the complex, which was titrated with a 1×10^{-2} M solution of the tetrabutylammonium salt. All spectrophotometric titration curves were fitted with the HYPERQUAD program.[30]

Table 4. Crystal data and structure refinement for compounds **1**–**4**.

	1	**2**	**3**	**4**
Formula	$C_{24}H_{36}Cl_2N_4O_{11}Zn$	$C_{28}H_{42}N_8O_9Zn$	$C_{26}H_{40}Cl_2N_4O_{12}Zn$	$C_{26}H_{40}N_6O_{10}Zn$
Molecular weight (g mol^{-1})	692.84	700.07	736.89	662.01
Crystal system	monoclinic	monoclinic	monoclinic	monoclinic
Space group	$P2_1/a$	$C2/c$	$P2_1$	$C2/c$
a [Å]	12.5098(13)	12.1074(12)	10.1909(2)	23.327(5)
b [Å]	12.6196(13)	16.0368(15)	14.9591(3)	9.081(5)
c [Å]	18.1259(18)	16.9168(17)	10.9007(2)	17.325(5)
β [°]	92.263(2)	91.604(2)	108.7440(10)	122.948(5)
Volume [Å^3]	2859.3(5)	3283.3(6)	1573.64(5)	3080(2)
F(000)	1440	1472	768	1392
Z	4	4	2	4
Temperature [K]	298(2)	298(2)	298(2)	298(2)
λ(Mo-K_α) [Å]	0.71073	0.71073	0.71073	0.71073
ρ_{calcd} [g cm^{-3}]	1.609	1.416	1.555	1.428
μ [mm^{-1}]	1.112	0.811	1.018	0.861
R_{int}	0.1536	0.0341	0.0285	0.0701
Measured reflections	19748	10295	11076	10351
Unique reflections	7095	3900	7223	3804
Observed reflections [$I > 2\sigma(I)$]	2544	2355	5542	2089
Goodness-of-fit on F^2	0.867	1.026	1.019	0.874
R_1 [$I > 2\sigma(I)$][a]	0.0632	0.0535	0.0447	0.0607
wR_2 (all data)[b]	0.1076	0.1640	0.1046	0.1748

[a] $R_1 = \Sigma||F_o| - |F_c||/\Sigma|F_o|$. [b] $wR_2 = \{\Sigma[w(||F_o|^2 - |F_c|^2)^2]/ \Sigma[w(F_o^4)]\}^{1/2}$.

X-ray crystallography: Crystal data and details on data collection and refinement are summarised in Table **4**. Three-dimensional X-ray data for compounds **1**–**4** were collected on a Bruker SMART 1000 CCD diffractometer by the φ-ω scan method. Reflections were measured from a hemisphere of data collected on frames each covering 0.3° in ω. Data were corrected for Lorentz and polarisation effects and for absorption by semi-empirical methods.[31] Complex scattering factors were taken from the program package SHELXTL[32] as implemented on a Pentium computer. The structures were solved by direct methods and refined by full-matrix least-squares on F^2. The hydrogen atoms were included in calculated positions and refined in riding mode, except for H(3A), H(3B), H(4A) and H(4B) in **1**, H(1N) and H(2N) in **2**, and H(1N), H(2N), H(3N) and H(4N) in **3**, which were first located in a Fourier difference density map and left to freely refine. Minimum and maximum final electron density of –0.370 and 0.474 Å^{-3} for **1**, –0.310 and 0.526 Å^{-3} for **2**, –0.508 and 0.343 Å^{-3} for **3**, and –0.545 and 0.668 Å^{-3} for **4** were found. The structure of **4** presents a disorder on an oxygen atom of the nitrate groups. The disorder has been resolved and two atomic sites have

been observed and refined with isotropic atomic displacement parameters. The site occupancy factor was 0.546 for O(1SA).

CCDC-614190 to -614193 contain the supplementary crystallographic data for this paper. These data can be obtained free of charge from The Cambridge Crystallographic Data Center via http://www.ccdc.cam.ac.uk/data_request/cif.

DFT studies: All calculations were performed using the Gaussian 03 (Revision C.01)[33] program package with the B3LYP[34,35] three-parameter hybrid density functional, unless otherwise stated. In vacuo geometry optimisations of the $[Zn(L^1)]^{2+}$, $[Zn(L^2)]^{2+}$ and $[Zn(L^2)(NO_3)_2]$ systems were performed without constraints by using the Ahlrichs' valence triple-ζ (VTC)[22] basis set on Zn and the standard 6-31G(d) basis set on C, H, N and O atoms. The X-ray crystal structures of compounds **1**, **3** and **4** were used as input for geometry optimisations. The stationary points found on the potential energy surfaces as a result of the geometry optimisations have been tested to represent energy minima rather than saddle points by frequency analysis. Binding energies of the macrocyclic ligands were calculated as $E_{bind} = E_{metal\ complex} - (E_{cation} + E_{free\ ligand})$, with the free ligand at the geometry found within the complex. Therefore, calculated binding energies are static and do not include energy contributions because of changes in ligand geometry. The binding energy (of the macrocyclic ligand) in $[Zn(L^2)(NO_3)_2]$ was calculated as $E_{bind} = E_{metal\ complex} - (E^{Zn(NO_3)_2} + E_{free\ ligand})$. Basis Set Superposition Errors (BSSEs) were calculated using the Counterpoise method.[26] BSSE is an undesirable consequence of using finite basis sets that leads to an overestimation of the binding energy.

Supporting information

In vacuo optimised Cartesian Coordinates [Å], Table S1 listing experimental and calculated angles of the metal coordination environment for the [Zn(L1)]2+, [Zn(L2)]2+ and [Zn(L2)(NO3)2] systems, and Figures S1, S2 and S3. See also the footnote on the last page of this article.

Acknowledgements

The authors thank Xunta de Galicia (PGIDIT03TAM10301PR) and Universidade da Coruña for generous financial support. The authors are indebted to Centro de Supercomputación of Galicia (CESGA) for providing the computer facilities.

References

[1] G. W. Gokel, *Crown Ethers and Cryptands*, RSC, Cambridge, **1991**.

[2] S. R. Cooper, *Crown Compounds: Toward Future Applications*, VCH Verlagsgesellschaft, Weinheim, **1992**.

[3] F. Vögtle, *Supramolecular Chemistry*, John Wiley & Sons, Chichester, **1991**.

[4] C. J. Pedersen, J.-M. Lehn, D. J. Cram, *Resonance* **2001**, *6*, 71–79.

[5] N. Steinke, W. Frey, A. Baro, S. Laschat, C. Drees, M. Nimtz, C. Haegele, F. Giesselmann, *Chem. Eur. J.* **2006**, *12*, 1026–1035.

[6] J. R. Pfeifer, P. Reiss, U. Koert, *Angew. Chem. Int. Ed.* **2006**, *45*, 501–504.

[7] a) G. W. Gokel, S. H. Korzeniowski in *Macrocyclic Polyether Synthesis*, Springer, Berlin,**1982**, pp. 6, 39. b) Y. Nakatsuji, T. Nakamura, M. Yometani, H. Yuya, M. Okahara, *J. Am. Chem. Soc.* **1988**, *110*, 531.

[8] G. W. Gokel, *Chem. Soc. Rev.* **1992**, *21*, 39–47 and references cited therein.

[9] C. Platas-Iglesias, L. Vaiana, D. Esteban-Gómez, F. Avecilla, J. A. Real, A. de Blas, T. Rodríguez-Blas, *Inorg. Chem.* **2005**, *44*, 9704–9713.

[10] C. Rodríguez-Infante, D. Esteban, F. Avecilla, A. de Blas, T. Rodríguez-Blas, J. Mahía, A. L. Macedo, C. F. G. C. Geraldes, *Inorg. Chim. Acta* **2001**, *317*, 190–198.

[11] L. Vaiana, C. Platas-Iglesias, D. Esteban-Gómez, F. Avecilla, J. M. Clemente-Juan, J. A. Real, A. de Blas, T. Rodríguez, *Dalton Trans.* **2005**, 2031–2037.

[12] K. Nakamoto, *Infrared and Raman Spectra of Inorganic and Coordination Compounds*, 3rd ed., John Wiley & Sons, New York, Chichester, Brisbane, Toronto, **1972**, pp. 142–154.

[13] K. M. Doxsee, J. R. Hagadorn, T. J. R. Weakley, *Inorg. Chem.* **1994**, *33*, 2600–2606.

[14] O. Schlager, K. Wieghardt, H. Grondey, A. Rufinska, B. Nuber, *Inorg. Chem.* **1995**, *34*, 6440–6448.

[15] K. R. Adam, S. P. H. Arshad, D. S. Baldwin, P. A. Duckworth, A. J. Leong, L. F. Lindoy, B. J. McCool, M. McPartlin, B. A. Tailor, P. A. Tasker, *Inorg. Chem.* **1994**, *33*, 1194–1200.

[16] A. Looney, G. Parkin, *Inorg. Chem.* **1994**, *33*, 1234–1237.

[17] C.-D. Wu, C.-Z. Lu, W.-B. Yang, H.-H. Zhuang, J.-S. Huang, *Inorg. Chem.* **2002**, *41*, 3302–3307.

[18] A. Kirkpatrick, W. T. A. Harrison, *Solid State Sci.* **2004**, *6*, 593–598.

[19] W. J. Weary, *Coord. Chem. Rev.* **1971**, *7*, 81–122.

[20] C. S. Wilcox, *Frontiers in Supramolecular Chemistry and Photochemistry*, VCH Verlagsgesellschaft, Weinheim, **1991**, 123–143.

[21] L. F. Lindoy, T. Rambusch, B. W. Skelton, A. H. White, *J. Chem. Soc., Dalton Trans.* **2001**, 1857–1862.

[22] A. Schäfer, H. Horn, R. Ahlrichs, *J. Chem. Phys.* **1992**, *97*, 2571–2577.

[23] A. A. Palacios, P. Alemany, S. Alvarez, *Inorg. Chem.* **1999**, *38*, 707–715.

[24] M. R. Willcott, R. E. Lenkinski, R. E. Davis, *J. Am. Chem. Soc.* **1972**, *94*, 1742–1744.

[25] R. E. Davis, M. R. Willcott, *J. Am. Chem. Soc.* **1972**, *94*, 1744–1745.

[26] S. F. Boys, F. Bernardi, *Mol. Phys.* **1970**, *19*, 553–566.

[27] I. Yoon, J. Seo, J.-E. Lee, K.-M. Park, J. S. Kim, M. S. Lah, S. S. Lee, *Inorg. Chem.* **2006**, *45*, 3487–3489.

[28] D. Esteban, D. Bañobre, A. de Blas, T. Rodríguez-Blas, R. Bastida, A. Macías, A. Rodríguez, D. E. Fenton, H. Adams, J. Mahía, *Eur. J. Inorg. Chem.* **2000**, 1445–1456.

[29] W. C. Wolsey, *J. Chem. Educ.* **1973**, *50*, A335–A337.

[30] P. Gans, A. Sabatini, A. Vacca, *Talanta* **1996**, *43*, 1739–1753.

[31] *SADABS Area-Detector Absorption Correction*, Siemens Industrial Automation, Inc., Madison, WI, **1996**.

[32] G. M. Sheldrick, *SHELXTL Bruker Analytical X-ray System*, release 5.1, Madison, WI, **1997**.

[33] M. J. Frisch, G. W. Trucks, H. B. Schlegel, G. E. Scuseria, M. A. Robb, J. R. Cheeseman, J. A. Montgomery Jr, T. Vreven, K. N. Kudin, J. C. Burant, J. M. Millam, S. S. Iyengar, J. Tomasi, V. Barone, B. Mennucci, M. Cossi, G. Scalmani, N. Rega, G. A. Petersson, H. Nakatsuji, M. Hada, M. Ehara, K. Toyota, R. Fukuda, J. Hasegawa, M. Ishida, T. Nakajima, Y. Honda, O. Kitao, H. Nakai, M. Klene, X. Li, J. E. Knox, H. P. Hratchian, J. B. Cross, C. Adamo, J. Jaramillo, R. Gomperts, R. E. Stratmann, O. Yazyev, A. J. Austin, R. Cammi, C. Pomelli, J. W. Ochterski, P. Y. Ayala, K. Morokuma, G. A. Voth, P. Salvador, J. J. Dannenberg, V. G. Zakrzewski, S. Dapprich, A. D. Daniels, M. C. Strain, O. Farkas, D. K. Malick, A. D. Rabuck, K. Raghavachari, J. B. Foresman, J. V. Ortiz, Q. Cui, A. G. Baboul, S. Clifford, J. Cioslowski, B. B. Stefanov, G. Liu, A. Liashenko, P. Piskorz, I. Komaromi, R. L. Martin, D. J. Fox, T. Keith, M. A. Al-Laham, C. Y. Peng, A. Nanayakkara, M. Challacombe, P. M. W. Gill, B. Johnson, W. Chen, M. W. Wong, C. Gonzalez, J. A. Pople, Gaussian, Inc., Wallingford, CT, **2004**.

[34] A. D. Becke, *J. Chem. Phys.* **1993**, *98*, 5648–5652.

[35] C. Lee, W. Yang, R. G. Parr, *Phys. Rev. B* **1988**, *37*, 785–789.

[i] Supporting information for this article is available online: https://doi.org/10.1002/ejic.200601012.